Journal of The Electrochemical Society, **153** (8) A1604-A1609 (2006)
0013-4651/2006/153(8)/A1604/6/$20.00 © The Electrochemical Society

Proton Conduction in In^{3+}-Doped SnP_2O_7 at Intermediate Temperatures

Masahiro Nagao,[a,*] Toshio Kamiya,[a] Pilwon Heo,[a] Atsuko Tomita,[b] Takashi Hibino,[a,,z] and Mitsuru Sano[a]**

[a]*Graduate School of Environmental Studies, Nagoya University, Chikusa-ku, Nagoya 464-8601, Japan*
[b]*Materials Research Institute for Sustainable Development, National Institute of Advanced Industrial Science and Technology, Moriyama-ku, Nagoya 463-8560, Japan*

SnP_2O_7-based proton conductors were characterized by Fourier transform infrared spectroscopy (FTIR), temperature-programmed desorption (TPD), X-ray diffraction (XRD), and electrochemical techniques. Undoped SnP_2O_7 showed overall conductivities greater than 10^{-2} S cm^{-1} in the temperature range of 75–300°C. The proton transport numbers of this material at 250°C under various conditions were estimated, based on the ratio of the electromotive force of the galvanic cells to the theoretical values, to be 0.97–0.99 in humidified H_2 and 0.89–0.92 under fuel cell conditions. Partial substitution of In^{3+} for Sn^{4+} led to an increase in the proton conductivity (from 5.56×10^{-2} to 1.95×10^{-1} S cm^{-1} at 250°C, for example). FTIR and TPD measurements revealed that the effects of doping on the proton conductivity could be attributed to an increase in the proton concentration in the bulk $Sn_{1-x}In_xP_2O_7$. The deficiency of P_2O_7 ions in the $Sn_{1-x}In_xP_2O_7$ bulk decreased the proton conductivity by several orders of magnitude, which was explained as due to a decrease in the proton mobility rather than the proton concentration. The mechanism of proton incorporation and conduction is examined and discussed in detail.
© 2006 The Electrochemical Society. [DOI: 10.1149/1.2210669] All rights reserved.

Manuscript submitted November 14, 2005; revised manuscript received January 9, 2006. Available electronically June 15, 2006.

Nafion is widely viewed as the most important proton-conducting electrolyte material in polymer electrolyte fuel cells.[1] In recent years, however, there has been considerable interest in the development of alternative materials with high proton conductivities at operating temperatures of 150°C or more.[2] At intermediate temperatures, CO poisoning of the platinum catalyst becomes less serious compared to lower temperatures, so that the fuel cell system does not require a CO removal unit (water-gas shift and CO preferential oxidation reactors). In addition, the electrode reaction kinetics is enhanced, and water is easily desorbed from the cathode.

Several approaches have been proposed for the design of intermediate-temperature proton conductors.[3-9] Although a number of hydrous proton conductors have been developed, most of them require highly humid conditions to achieve sufficient proton conductivities.[10] Anhydrous proton conductors, at least in principle, do not require the presence of water as the charge carrier, because protons migrate via jumps between adjacent oxide ions by a series of making and breaking of hydrogen bonds (Grotthuss or hopping mechanism). However, the proton conductivities reported so far were in the range of 10^{-2} S cm^{-1}, which is not sufficiently high to provide good fuel cell performance.[5,11,12]

We have recently reported that an anhydrous proton conductor, 10 mol % In^{3+}-doped SnP_2O_7 ($Sn_{0.9}In_{0.1}P_2O_7$), shows high proton conductivities $>10^{-1}$ S cm^{-1} between 150 and 350°C under water-free conditions.[13] Attempts to apply this material as an electrolyte in some electrochemical devices were also made. A fuel cell using the 0.35 mm thick $Sn_{0.9}In_{0.1}P_2O_7$ electrolyte membrane yielded a power density of 264 mW cm^{-2} under unhumidified H_2/air conditions.[13] In addition, an electrochemical reactor using the $Sn_{0.9}In_{0.1}P_2O_7$ electrolyte membrane with a PtBa/C cathode reduced NO_x to N_2 with a current efficiency of 5.81% at 250°C in oxidizing atmospheres (p_{O_2} = 0.02–0.09 atm).[14] This material also had the potential to be used for NO_x and other gas sensor applications.[15] However, a detailed mechanism of the incorporation of protons in the bulk is still unclear. Moreover, the migration of protons through the electrolyte is not well understood.

The purpose of this study was to attempt to address the above questions and clarify the mechanisms. Proton conduction in undoped SnP_2O_7 was first characterized by impedance spectra, the H/D isotope effect, and galvanic cell measurements. The effects of In^{3+} doping and P_2O_7 deficiency on the proton conductivity were then clarified by Fourier transform infrared spectroscopy (FTIR) and temperature-programmed desorption (TPD) techniques. A mechanism of proton incorporation and conduction is proposed on the basis of these results.

Experimental

MP_2O_7 (M = Si, Ge, Sn, and Ti) was prepared as follows. The corresponding oxide (SiO_2, GeO_2, SnO_2, or TiO_2) was mixed with 85% H_3PO_4 and then held with stirring at 300°C until it formed a paste with a high viscosity. The pastes were calcined in an alumina pot at 650°C for 2.5 h and then ground with a mortar and pestle. $Sn_{1-x}In_x(P_2O_7)_{1-y}$ was also synthesized in a similar manner from SnO_2, In_2O_3, and 85% H_3PO_4. In this case, the x and y values were changed by varying the molar ratio of the raw materials. The preparation of layered SnP_2O_7 and amorphous $Sn_2P_2O_7$ has been described in the literature.[16,17] The final P/M or P/(Sn + In) molar ratio of the compounds was confirmed to be 2.0 (±0.02) from X-ray fluorescence (XRF) measurements. The crystalline structure of the compounds was measured using X-ray diffraction (XRD). The lattice constant measurements for SnP_2O_7 and $Sn_{1-x}In_xP_2O_7$ were made using an Si internal standard.

For electrochemical measurements, the compound powders were pressed into pellets (diameter 12 mm, thickness 1.0–1.2 mm) under a pressure of 2×10^3 kg cm^{-2}. The ac conductivity values of the pellets were measured by the standard four-probe method in different atmospheres (p_{H_2O} = 0.0008–0.12 atm; p_{O_2} = 10^{-27}–1 atm). The frequency range was 0.1–10^6 Hz, and the ac amplitude was 10 mV. The dc conductivity values were also estimated from the IR drop of the pellet measured by current interruption method. Two types of galvanic cells, a H_2 concentration cell and a H_2/air fuel cell, were fabricated using the pellet (thickness ~1.2 mm, diameter 12 mm) as the electrolyte membrane. Both anode and cathode (area 0.5 cm^2) were made from the catalyst (10 wt % Pt/C, E-TEK) and carbon paper (Toray TGPH-090), wherein the Pt loading was 0.6 mg cm^{-2}. The electromotive forces (emfs) of the galvanic cells were monitored as a function of the gas concentration or temperature.

FTIR spectra of SnP_2O_7 and $Sn_{0.9}In_{0.1}(P_2O_7)_{1-y}$ powders were measured in the range of 400–4000 cm^{-1} in a JASCO FT/IR-460 Plus spectrometer. FTIR measurements were performed in the transmission mode by the KBr pellet technique. Data points were obtained in 60 scans with a resolution of 4 cm^{-1}.

* Electrochemical Society Student Member.
** Electrochemical Society Active Member.
z E-mail: hibino@urban.env.nagoya-u.ac.jp

Downloaded on 2013-08-25 to IP 133.6.32.9 address. Redistribution subject to ECS license or copyright; see ecsdl.org/site/terms_use

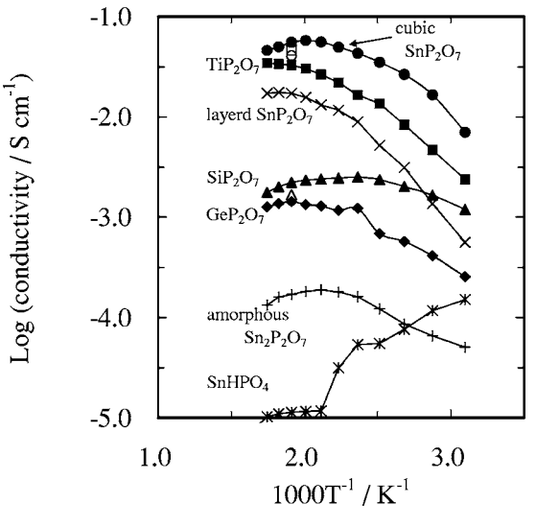

Figure 1. Temperature dependence of the conductivity of MP_2O_7 (M = Si, Ge, Sn, and Ti) in unhumidified air (p_{H_2O} = ~ 0.0075 atm). Symbols as noted in figure.

TPD spectra of the $Sn_{0.9}In_{0.1}(P_2O_7)_{1-y}$ powders were measured in a conventional TPD apparatus with an on-line mass spectrometer.[18] Sample powder (4 g) was heated in a stream of humidified Ar at 200°C for 2 hours. After purging with dry Ar, the sample powder was heated at a rate of 5°C min^{-1} until the evolution of gases was completed.

Results and Discussion

Proton conduction in undoped SnP_2O_7.— Figure 1 shows the temperature dependence of the conductivity of cubic MP_2O_7(M = Si, Ge, Sn, and Ti) in unhumidified air (p_{H_2O} = ~ 0.0075 atm). The conductivity increased in the order of $Ge^{4+} < Si^{4+} < Ti^{4+} < Sn^{4+}$, which agreed with the closely related order of electron-hole conductivity for the species (as discussed later). However, Matsui et al. reported conductivities of SiP_2O_7 and TiP_2O_7 much lower than those shown in Fig. 1.[19] The dc conductivity measurements for SnP_2O_7, TiP_2O_7, and SiP_2O_7 were made to prove the validity of our results. The conductivities measured at 250°C were 4.7×10^{-1}, 4.6×10^{-2}, and 1.7×10^{-3} S cm^{-1} for SnP_2O_7, TiP_2O_7, and SiP_2O_7, respectively, which were in agreement with their ac conductivities shown in Fig. 1. As mentioned later, the conductivity of MP_2O_7 was significantly decreased by the deficiency of P_2O_7 ions in the lattice. It is thus speculated that the samples prepared by Matsui et al. may lose a slight amount of $P_2O_7^{4-}$ ions by the vaporization of phosphorus species during the preparation process at 700°C, resulting in the low conductivities of SiP_2O_7 and TiP_2O_7.

Other P_2O_7-based tin phosphates are known, including layered SnP_2O_7 and amorphous $Sn_2P_2O_7$. As can be seen from Fig. 1, the conductivities of these materials were higher than those of PO_4-based $SnHPO_4$ but lower than those of cubic SnP_2O_7, indicating the importance of the crystalline structure, not only based on the P_2O_7 groups but also on cubic symmetry. These results also suggest that the conductivity of SnP_2O_7 is related to bulk conduction rather than surface conduction, because the former is more strongly influenced by structural characteristics than the latter.

Comparison of the emf values of the following galvanic cells with the theoretical values calculated from Nernst's equation was performed to estimate the proton transport number of SnP_2O_7 under various conditions

$$H_2(1\ atm), Pt/C|SnP_2O_7|Pt/C, H_2 + Ar(0.1\ atm) \quad [1]$$

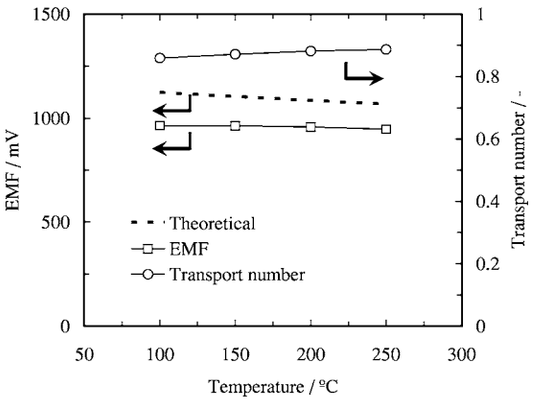

Figure 2. EMF values of galvanic cells using SnP_2O_7 as an electrolyte. H_2 (1 atm) and H_2 balanced with Ar were supplied to the anode and cathode, respectively. The operating temperatures were from 100 to 250°C.

$$H_2, Pt/C|SnP_2O_7|Pt/C, air \quad [2]$$

It can be seen from Fig. 2 that all the emf values observed for cell 1 between 100 and 250°C were very close to the corresponding theoretical values. From the ratio of the emf value to the theoretical value, the proton transport number of SnP_2O_7 was calculated to be in the range 0.97–0.99, which means that this material is substantially a pure proton conductor in H_2 atmospheres. Cell 2 showed emf values deviating from the theoretical values (proton transport number = 0.89–0.92), although the EMF values were as high as ~920 mV. This deviation was due to electron holes in the SnP_2O_7 bulk (as described later). However, mechanical leakage of gas through the electrolyte may also be responsible for the lower emf values compared to the theoretical values, because the EMF value was affected by the thickness of the electrolyte used. For example, the EMF value increased from 922 to 934 mV with increasing electrolyte thickness from 1.2 to 2.6 mm.

SnP_2O_7 nominally does not contain protons in the bulk. Therefore, we attempted to clarify how this material is protonated. The dependence of the overall conductivity of SnP_2O_7 on the partial pressure of oxygen (p_{O_2}) was investigated at various p_{H_2O} values. As shown in Fig. 3, at p_{H_2O} = 0.0008 atm, a large increase in conductivity with increasing p_{O_2} was observed under oxidizing conditions (p_{O_2} = 0.21–1 atm), indicating that this material shows mixed

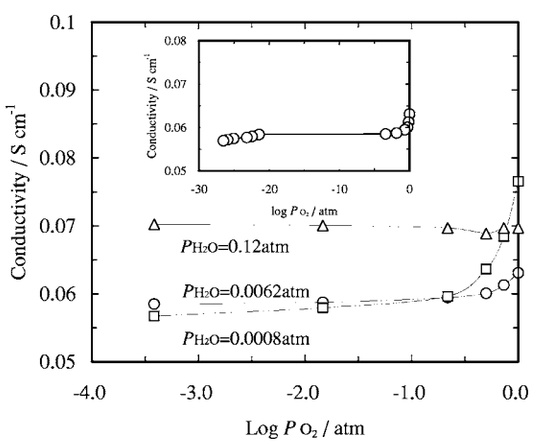

Figure 3. p_{O_2} dependence of conductivity of SnP_2O_7 at 250°C. p_{H_2O} of 0.0008, 0.0062, and 0.12 atm were controlled by passing the gases through dry ice–ethanol (−72°C), ice (0°C), and warmed water (50°C) baths, respectively.

Downloaded on 2013-08-25 to IP 133.6.32.9 address. Redistribution subject to ECS license or copyright; see ecsdl.org/site/terms_use

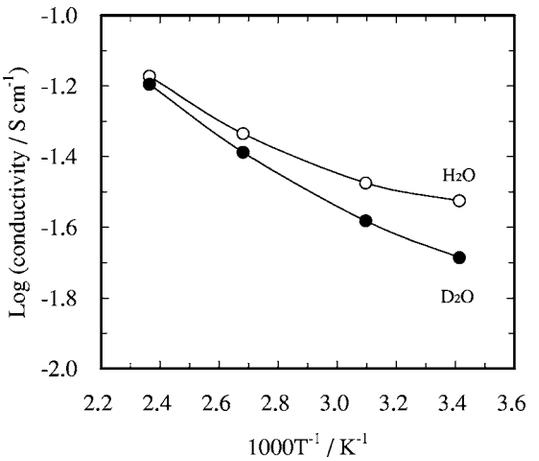

Figure 4. Isotope effect on conductivity of SnP_2O_7. The data were obtained in argon saturated with H_2O or D_2O vapor at 20°C. The transient change in ohmic resistance was measured at 50°C.

electron-hole and proton conduction. However, such a tendency decreased with increasing p_{H_2O}. In particular, at p_{H_2O} = 0.12 atm, the conductivity was almost independent of p_{O_2}, indicating the disappearance of electron holes from the bulk. It appears that there is interaction between water vapor and electron holes. The following equilibrium has been proposed as a mechanism of proton incorporation in perovskite oxides such as $SrCe_{0.95}Yb_{0.05}O_{3-\alpha}$[20]

$$H_2O + 2h^{\cdot} \rightarrow 2H^{\cdot} + \tfrac{1}{2}\,O_2$$

$$\left(H_2O + 2\,O_o^x + 2h^{\cdot} \rightarrow 2OH_o^{\cdot} + \tfrac{1}{2}\,O_2\right) \qquad [3]$$

Here, $h^{\cdot}$ and $H^{\cdot}$ denote an electron hole and a proton, respectively. It is reasonable to consider that protons are formed in the SnP_2O_7 bulk through Reaction 3. We similarly measured the electron-hole conductivity for other MP_2O_7 and found it to be an order of magnitude, in agreement with the proton conductivity measurements. This result supports the validity of Reaction 3. Another important result in Fig. 3 is that almost no variation of the conductivity with p_{O_2} under reducing conditions (p_{O_2} = $\sim 10^{-20}$–10^{-27} atm) was observed, excluding the reduction of Sn^{4+} and P^{5+} to lower valences.

We also attempted to develop a more detailed explanation for proton conduction in the SnP_2O_7 bulk. An H/D isotope effect on conductivity is helpful to clarify this point, and the results are shown in Fig. 4. SnP_2O_7 yielded a 1.06–1.44 times higher conductivity and a lower activation energy of 0.03 eV for H_2O-containing atmospheres than for D_2O-containing atmospheres. This result can be interpreted by a nonclassic H/D isotope effect.[21,22] When the dissociation of the O-H bond is a rate-determining step for proton conduction, the activation energy for D^+ is higher than that for H^+ by a difference in zero point energy of 0.05 eV, which is near the difference in activation energy shown above. It is thus proposed that protons migrate via dissociation of O-H bonds (hopping mechanism).

Effect of In^{3+} doping in $Sn_{1-x}In_xP_2O_7$ on proton conduction.— Figure 5 shows typical XRD patterns of undoped and In^{3+}-doped SnP_2O_7 measured at room temperature. The peaks observed for SnP_2O_7 were almost identical to those reported in the literature.[16] SnP_2O_7 has a cubic or pseudocubic structure, with SnO_6 octahedra and P_2O_7 units at the corners and the edges, respectively. $Sn_{1-x}In_xP_2O_7$ with In^{3+} content of not more than 10 mol % showed the same patterns as those of SnP_2O_7 and an increasing lattice constant with increasing In^{3+} content, 7.945 Å for SnP_2O_7 and 7.950 Å for $Sn_{0.9}In_{0.1}P_2O_7$. $Sn_{1-x}In_xP_2O_7$ with In^{3+} contents of 20 and

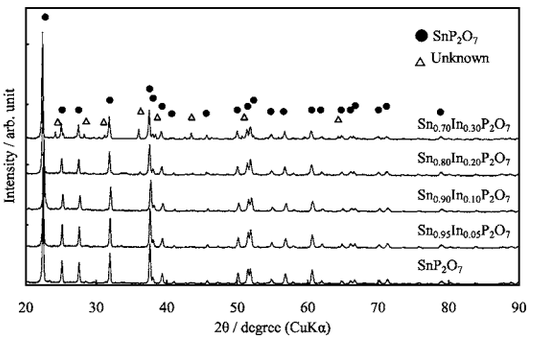

Figure 5. XRD patterns of $Sn_{1-x}In_xP_2O_7$.

30 mol % contained some other unidentified peaks. It seems that the In^{3+} content of 10 mol % is the limit of substitution for In^{3+}.

Proton conductivities for undoped and In^{3+}-doped SnP_2O_7 at different temperatures in unhumidified air (p_{H_2O} = $\sim$ 0.0075 atm) are shown in Fig. 6. The conductivity of $Sn_{1-x}In_xP_2O_7$ increased with increasing In^{3+} content and reached a maximum at In^{3+} = 10 mol %. This In^{3+} content of 10 mol % corresponded well with the substitution limit for In^{3+} estimated from the XRD measurements. Therefore, it is concluded that the doping of In^{3+} for Sn^{4+} plays an important role in the enhancement of proton conductivity. It should be noted here that the conductivities of undoped and In^{3+}-doped SnP_2O_7 increased monotonously with increasing temperature, which was different from "superprotonic" behavior that shows a sharp increase in the conductivity of some orders of magnitude by a structural transition from a low- to a high-temperature phase.[5,11,12,23] This is because SnP_2O_7 does not show such a structural transition in the temperature range of interest.[16] $Sn_{0.9}In_{0.1}P_2O_7$ with the highest conductivity of 1.95×10^{-1} S cm^{-1} at 200°C was used in subsequent experiments.

To better understand the effects of In^{3+} doping, the environment of the protons in the bulk $Sn_{0.9}In_{0.1}P_2O_7$ was observed by FTIR. An IR spectrum of $Sn_{0.9}In_{0.1}P_2O_7$ is shown in Fig. 7 along with the spectrum for undoped SnP_2O_7 for comparison. In both IR spectra, some absorption bands appeared from 1560 to 3720 cm^{-1}, with large differences in the absorbance between the two materials. The wide absorption bands centered at 1655 and 3410 cm^{-1} are evidence

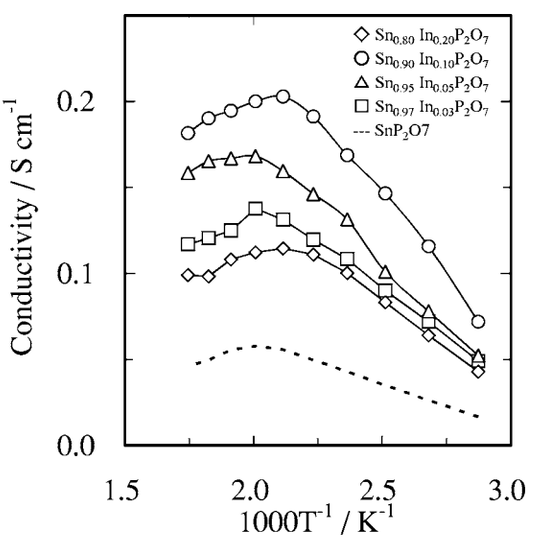

Figure 6. Temperature dependence of the conductivity of $Sn_{1-x}In_xP_2O_7$. The samples were maintained in unhumidified air (p_{H_2O} = $\sim$ 0.0075 atm).

Downloaded on 2013-08-25 to IP 133.6.32.9 address. Redistribution subject to ECS license or copyright; see ecsdl.org/site/terms_use

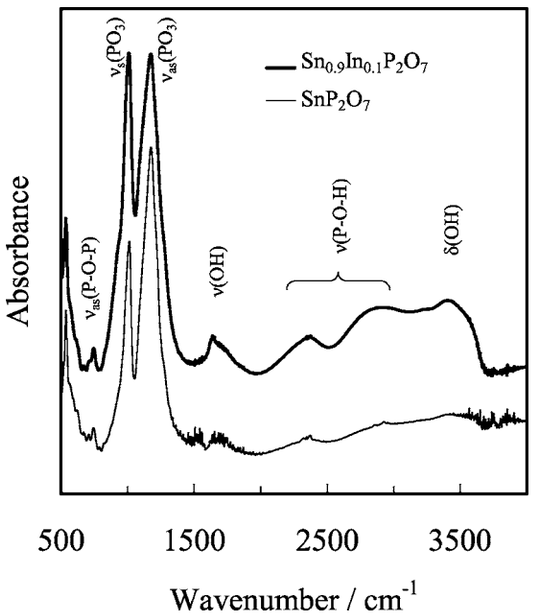

Figure 7. IR spectra of SnP_2O_7 and $Sn_{0.9}In_{0.1}P_2O_7$.

of υ(OH) and δ(OH), respectively.[24-26] The absorbance ratios of $Sn_{0.9}In_{0.1}P_2O_7$ to SnP_2O_7 were 5.2 and 5.7 for υ(OH) and δ(OH), respectively, which are comparable to their conductivity ratio of 4.6 at 50°C (Fig. 6). While care should be taken to account for water adsorbed on the sample surface, these results at least suggest that the absorption bands are mainly attributable to protons incorporated in the bulk. It is also likely that the protons interact with the lattice oxide ions to form hydrogen bonds.

A more quantitative measurement of the proton concentration in $Sn_{0.9}In_{0.1}P_2O_7$ and SnP_2O_7 was made by TPD of hydrogen species. The TPD spectra are shown in Fig. 8. Water vapor and a small amount of H_2 were evolved from 260 to 1050°C. The evolution of water vapor from water adsorbed on the surface of the samples cannot be neglected, especially for data at relatively low temperatures. However, we determined the proton concentrations in $Sn_{0.9}In_{0.1}P_2O_7$ and SnP_2O_7 by assuming that all the evolved water vapor and H_2 can be attributed to the incorporated protons. The resulting proton concentration values were 10.4 and 2.5 mol % for $Sn_{0.9}In_{0.1}P_2O_7$ and SnP_2O_7, respectively. Note that the former value was in good agreement with the proton concentration predicted from

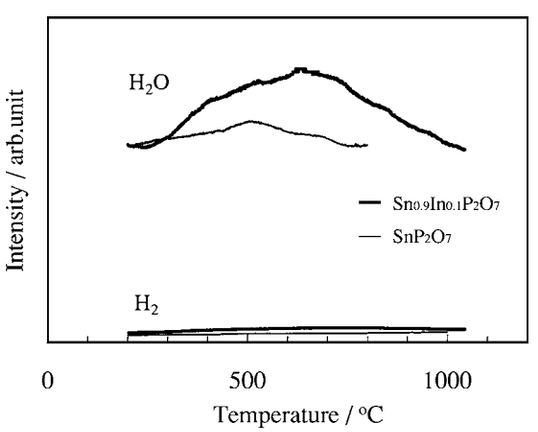

Figure 8. TPD spectra of SnP_2O_7 and $Sn_{0.9}In_{0.1}P_2O_7$.

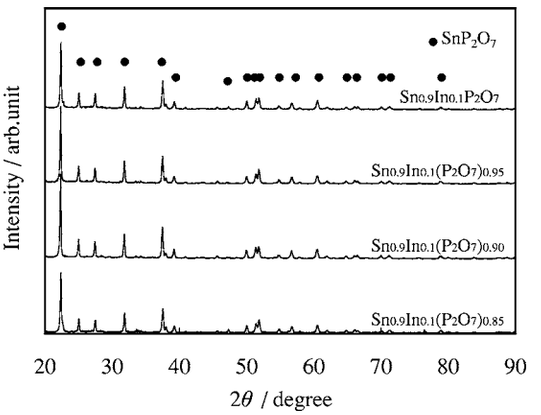

Figure 9. XRD patterns of $Sn_{0.9}In_{0.1}(P_2O_7)_{1-y}$.

the In^{3+} content of 10 mol %. It thus appears that the protons were fully introduced as point defects by the substitution of In^{3+} for Sn^{4+}.

Electron holes and oxygen vacancies are considered to be original positive defects in the $Sn_{0.9}In_{0.1}P_2O_7$ bulk. As described previously, protons are incorporated into the bulk according to Reaction 3. Another possible reaction is the following interaction between water vapor and an oxygen vacancy[20]

$$H_2O(g) + V\ddot{o} \rightarrow 2H_i + O_o^x$$

$$[H_2O(g) + O_o^x + V\ddot{o} \rightarrow 2OH_o] \qquad [4]$$

Here, Vö and O_o^x denote an oxygen vacancy and a lattice oxide ion, respectively. The degree of Reaction 4 cannot be entirely demonstrated at this stage. However, when the proton conductivity of $Sn_{0.9}In_{0.1}P_2O_7$ was measured at different p_{H_2O} values at 250°C, it slightly increased with increasing p_{H_2O}. This result is associated with the process of proton incorporation through Reaction 4 rather than 3, because the order of mobility is oxygen vacancy < proton < electron hole. Therefore, Reaction 4 as well as Reaction 3 are possible mechanisms of proton incorporation.

Effects of P_2O_7 deficiency in $Sn_{0.9}In_{0.1}P_2O_7$ on proton conduction.— P_2O_7-deficient $Sn_{0.9}In_{0.1}(P_2O_7)_{1-y}$ with y values of 0–0.15 was synthesized. Figure 9 shows the results of XRD measurements for $Sn_{0.9}In_{0.1}(P_2O_7)_{1-y}$. The XRD data showed similarities in the peak position and intensity among the various $Sn_{0.9}In_{0.1}(P_2O_7)_{1-y}$ samples and an increase in the full width at half maximum (fwhm) with the amount of P_2O_7 deficiency. For example, the fwhm's for the (200) reflection of $Sn_{0.9}In_{0.1}P_2O_7$ and $Sn_{0.9}In_{0.1}(P_2O_7)_{0.85}$ were 0.192–0.200°, respectively. These results suggest substantial distortion and disorder of the crystalline structure of $Sn_{0.9}In_{0.1}(P_2O_7)_{1-y}$. A significant decrease in the conductivity with P_2O_7 deficiency can be seen in Fig. 10. The proton conductivity of $Sn_{0.9}In_{0.1}(P_2O_7)_{0.85}$ was about 2 orders of magnitude lower than that of $Sn_{0.9}In_{0.1}P_2O_7$, indicating that the conductivity is strongly affected by the number of $P_2O_7^{4-}$ ions in the lattice.

FTIR measurements of $Sn_{0.9}In_{0.1}(P_2O_7)_{0.85}$ were conducted to clarify the effect of P_2O_7 deficiency on the proton conductivity. As shown in Fig. 11, the IR spectrum showed large peaks at almost the same wave numbers as those observed for $Sn_{0.9}In_{0.1}P_2O_7$. The absorbance ratios of $Sn_{0.9}In_{0.1}P_2O_7$ to $Sn_{0.9}In_{0.1}(P_2O_7)_{0.85}$ were 1.4 and 1.5 for υ(OH) and δ(OH), respectively, which are much smaller than their conductivity ratio shown in Fig. 10. A similar behavior was obtained for the TPD spectra, as shown in Fig. 12. The proton concentration in $Sn_{0.9}In_{0.1}(P_2O_7)_{0.85}$ was estimated to be about 8.1 mol % per unit, which is not significantly different from the value of 10.4 mol % observed for $Sn_{0.9}In_{0.1}P_2O_7$. Therefore, it is suggested that the large difference in proton conductivity between

Downloaded on 2013-08-25 to IP 133.6.32.9 address. Redistribution subject to ECS license or copyright; see ecsdl.org/site/terms_use

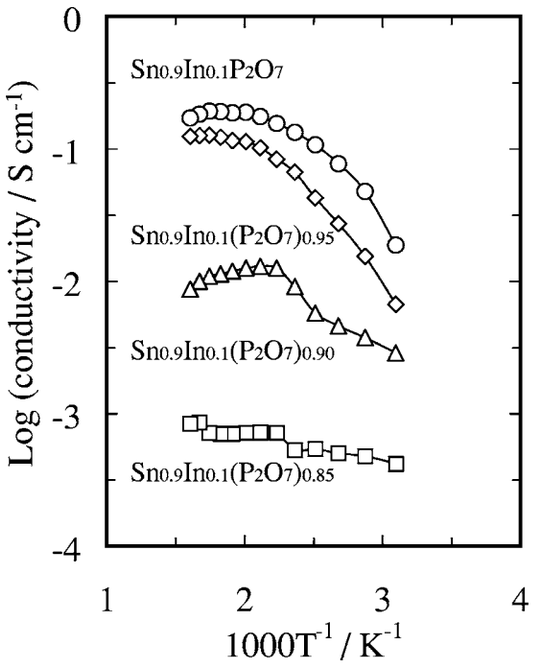

Figure 10. Temperature dependence of conductivity of $Sn_{0.9}In_{0.1}(P_2O_7)_{1-y}$. The samples were maintained in unhumidified air (p_{H_2O} = ~ 0.0075 atm).

$Sn_{0.9}In_{0.1}P_2O_7$ and $Sn_{0.9}In_{0.1}(P_2O_7)_{0.85}$ can be attributed to the difference in proton mobilities rather than proton concentrations between them. The proton conductivity, σ_H, is generally defined as follows[27]

$$\sigma_H = F\mu_H[H^{\cdot}]/v \qquad [5]$$

Here, σ_H, F, μ_H, $[H^{\cdot}]$, and v denote the proton conductivity, Faraday's constant, mobility of a proton, proton concentration, and molar volume of $Sn_{0.9}In_{0.1}P_2O_7$, respectively. The proton mobilities in $Sn_{0.9}In_{0.1}P_2O_7$ and $Sn_{0.9}In_{0.1}(P_2O_7)_{0.85}$ were calculated to be 1.49×10^{-3} and 6.3×10^{-6} $cm^2\ s^{-1}\ V^{-1}$, respectively. Considering the

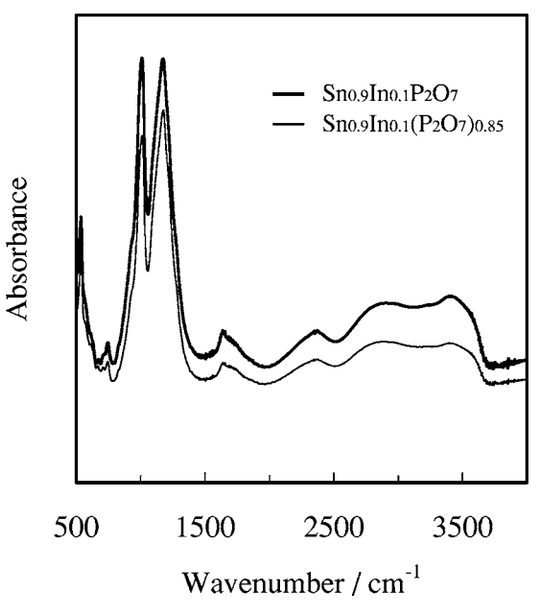

Figure 11. IR spectra of $Sn_{0.9}In_{0.1}P_2O_7$ and $Sn_{0.9}In_{0.1}(P_2O_7)_{0.85}$.

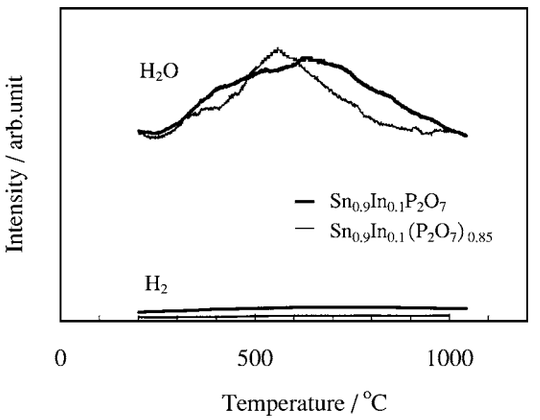

Figure 12. TPD spectra of $Sn_{0.9}In_{0.1}P_2O_7$ and $Sn_{0.9}In_{0.1}(P_2O_7)_{0.85}$.

results from the XRD and FTIR measurements, it is assumed that the extremely low proton mobility in $Sn_{0.9}In_{0.1}(P_2O_7)_{0.85}$ is not associated with the local environment of the protons in the crystalline lattice but is correlated with the long-range nature for the proton transfer between the crystalline lattices. This assumption is supported by the strong dependence of the proton conductivity on the crystalline structure of the P_2O_7-based tin phosphates with different types of P_2O_7 networks shown in Fig. 1. Thus, a possible speculation on the proton mobility of $Sn_{0.9}In_{0.1}(P_2O_7)_{0.85}$ is that the P_2O_7 deficiency causes a partial disconnection of the P_2O_7 network for proton conduction, resulting in a large energy barrier for proton jumps between sites.

Conclusions

Proton conduction in In^{3+}-doped SnP_2O_7 was investigated by controlling the In^{3+} and $P_2O_7^{4-}$ content in the bulk. SnP_2O_7 had an ionic transport number of ~1 and exhibited a large H/D isotope effect on conductivity, which demonstrates that the protons are migrating via a hopping mechanism. The substitution of In^{3+} for Sn^{4+} increased the proton concentration in the bulk, resulting in an increase in proton conductivity. The P_2O_7 deficiency caused extremely low proton conductivity, which was explained by a large increase in energy barrier for proton conduction due to partial disconnection of the P_2O_7 network for proton conduction.

Nagoya University assisted in meeting the publication costs of this article.

References

1. K. D. Kreuer, *Solid State Ionics*, **97**, 1 (1997).
2. T. Norby, *Solid State Ionics*, **125**, 1 (1999).
3. T. Kenjo and Y. Ogawa, *Solid State Ionics*, **76**, 29 (1995).
4. T. Matsui, S. Takeshita, Y. Iriyama, T. Abe, M. Inaba, and Z. Ogumi, *Electrochem. Commun.*, **6**, 180 (2004).
5. S. M. Haile, D. A. Boysen, C. R. I. Chisholm, and R. B. Merle, *Nature (London)*, **410**, 910 (2001).
6. W. Wieczorek, G. Zukowska, R. Borkowska, S. H. Chung, and S. Greenbaum, *Electrochim. Acta*, **46**, 1427 (2001).
7. A. Matsuda, T. Kanzaki, K. Tadanaga, M. Tatsumisago, and T. Minami, *Solid State Ionics*, **154–155**, 687 (2002).
8. J. D. Kim and I. Honma, *Electrochim. Acta*, **49**, 3179 (2004).
9. C. Yang, S. Srinivasan, A. B. Bocarsly, S. Tulyani, and J. B. Benziger, *J. Membr. Sci.*, **237**, 145 (2004).
10. G. Alberti and M. Casciola, *Solid State Ionics*, **145**, 3 (2001).
11. D. A. Boysen, T. Uda, C. R. I. Chisholm, and S. M. Haile, *Science*, **303**, 68 (2004).
12. T. Uda and S. M. Haile, *Electrochem. Solid-State Lett.*, **8**, A245 (2005).
13. M. Nagao, A. Takeuchi, P. Heo, T. Hibino, M. Sano, and A. Tomita, *Electrochem. Solid-State Lett.*, **9**, A105 (2006).
14. M. Nagao, T. Yoshii, T. Hibino, M. Sano, and A. Tomita, *Electrochem. Solid-State Lett.*, **9**, J1 (2006).
15. M. Nagao, Y. Namekata, T. Hibino, M. Sano, and A. Tomita, *Electrochem. Solid-State Lett.*, **9**, H48 (2006).
16. R. K. B. Gover, N. D. Withers, S. Allen, R. L. Withers, and J. S. O. Evans, *J. Solid State Chem.*, **166**, 42 (2002).

Downloaded on 2013-08-25 to IP 133.6.32.9 address. Redistribution subject to ECS license or copyright; see ecsdl.org/site/terms_use

17. M. Behm and J. T. S. Irvine, *Electrochim. Acta*, **47**, 1727 (2002).
18. T. Hibino, K. Mizutani, T. Yajima, and H. Iwahara, *Solid State Ionics*, **57**, 303 (1992).
19. T. Matsui, T. Kukino, R. Kikuchi, and K. Eguchi, in *Proceedings of the 31st Symposium on Solid State Ionics in Japan*, Niigata, Japan, Nov. 28–30, 2005, p. 52.
20. H. Iwahara, *Solid State Ionics*, **86–88**, 9 (1996).
21. T. Hibino, K. Mizutani, and H. Iwahara, *J. Electrochem. Soc.*, **140**, 2588 (1993).
22. N. Bonanos, *Solid State Ionics*, **145**, 265 (2001).
23. S. M. Haile, G. Lentz, K. D. Kreuer, and J. Maier, *Solid State Ionics*, **77**, 128 (1995).
24. P. S. Attidekou, P. A. Connor, P. Wormald, D. P. Tunstall, S. M. Francis, and J. T. S. Irvine, *Solid State Ionics*, **175**, 185 (2004).
25. H.-K. Lee, J.-I. Kim, J.-H. Park, and T.-H. Lee, *Electrochim. Acta*, **50**, 761 (2004).
26. Q. Wu, X. Sang, B. Liu, and V. G. Ponomareva, *Mater. Lett.*, **59**, 123 (2005).
27. H. Uchida, H. Yoshikawa, and H. Iwahara, *Solid State Ionics*, **35**, 229 (1989).

Downloaded on 2013-08-25 to IP 133.6.32.9 address. Redistribution subject to ECS license or copyright; see ecsdl.org/site/terms_use